Numerical and Experimental Study on Mechanism of Low Frequency Noise from Heat Recovery Steam Generator

Hongyun TANG[1], Weikang JIANG[2], Zhenmao ZHONG[3], Yingjiu ZHAO[4]

[1]Institute of Vibration, Shock and Noise, Shanghai Jiaotong University, China

[2]Huadian Heavy Industries Co., LTD., China

Abstract

The low frequency noise from heat recovery steam generator (HRSG) makes dominant contribution to the noise on the boundary of plant, which generation mechanism is investigated in this presentation. The non-stationary flow field and aeroacoustic noise is studied with hybrid numerical simulation, which is comprised of CFD method based on Large Eddy Simulation (LES) and acoustic analogy by using Ffowcs Williams-Hawkings equation. Models of cylindrical tube, fin-tube and tube array are established respectively to investigate the feature of vortex noise. The results of numerical simulation are compared with the acoustic intensities measured at the site. It can been understood from the simulation that the flow passing through the heat exchanger tube will induce vortex shedding, which results in the low frequency noise in HRSG. The vortex noise of a cylindrical tube lead to the obvious characteristic tone frequency as same as the vortex shedding frequency, but the spiral fin reduces the characteristic frequency and sound level. For the tube array of heat exchanger, due to the enhanced interaction of the flow field among tubes, the vortex noise is narrowband noise with some bandwidth. More targeted methods can be used for noise reduction of HRSG according to the research results.

Keywords: Heat recovery steam generator, aeroacoustic noise, vortex shedding

1. INTRODUCTION

As the development of urbanization process and the increase of electricity consumption, the construction of power plant utilizing gas-steam combined cycle becomes close to the residential area. The noise of power plant, especially the low frequency noise becomes an urgent issue. The Heat Recovery Steam Generator (HRSG) of power plant is the main object of noise control due to its large acoustic radiation area and stack. Researches on the mechanism of low frequency noise radiated from HRSG are relatively few, and some results indicated that the noise in HRSG is mainly composed of gas-turbine exhaust noise and heat exchanger tube array vortex noise, but which one is dominant has not been confirmed(1,2).

The on-site acoustic measurement was conducted at the HRSG of a gas-steam combined cycle power plant, and the results showed that the low frequency noise energy concentered at 63Hz octave band. The noise levels out of the wall was used to estimate the noise levels inside HRSG by reducing sound transmission loss. The HRSG noise and the gas-turbine exhaust noise are shown in Figure 1. From Figure 1, the heat exchanger tube array vortex noise rather than gas-turbine exhaust noise, might be the main sound source , especially for lower frequency components near 63Hz .

The flow passing through the heat exchanger tube array will induce vortex shedding. A lot of researches have been made on aerodynamics and aeroacoustics of flow around single cylinder and two cylinders in tandem arrangement and in staggered arrangement, but the effects of spiral fin on the vortex noise haven't drawn enough attention(3,4).

In this presentation, numerical simulation was carried out to analyze the non-stationary flow field

[1] cryth1989@sjtu.edu.cn
[2] wkjiang@sjtu.edu.cn
[3] zhongzm@chec.com.cn
[4] zhaoyj@chec.com.cn

and aeroacoustic noise of heat exchanger tube array using hybrid computation method. The CFD method based on Large Eddy Simulation (LES) and the acoustic analogy using Ffowcs Williams-Hawkings equation were employed. Models of cylindrical tube, fin-tube and tube array were established respectively to investigate the feature of vortex noise. The results of numerical simulation were compared with the acoustic intensities measured at the site to reveal the mechanism of low frequency in HRSG.

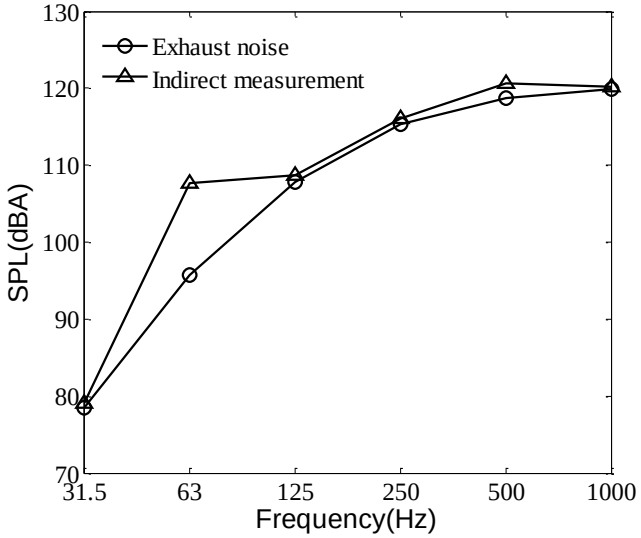

Figure 1 - Test results of the noise in HRSG

2. NUMERICAL ANALYSIS

The flow Mach number is lower than the incompressible flow limit, so the coupling effect between hydrodynamic field and sound field can be ignored. The numerical simulation adopts the hybrid computation method, consisting of CFD method based on Large Eddy Simulation (LES) and acoustic analogy using Ffowcs Williams-Hawkings equation(5).

2.1 Large Eddy Simulation

Considering the high Reynolds number and the low turbulent information, LES can balance computational cost and sufficient turbulent quantity at the same time. It deals with N-S equation using filter function:

$$\frac{\partial \bar{u}_i}{\partial t} + \frac{\partial \overline{u_i u_j}}{\partial x_j} = -\frac{1}{\rho}\frac{\partial \bar{p}}{\partial x_i} + \upsilon \frac{\partial^2 \bar{u}_i}{\partial x_j \partial x_j} \tag{1}$$

$$\frac{\partial \bar{u}_i}{\partial x_i} = 0 \tag{2}$$

where "—" denotes large scale components, u, p, ρ express velocity, pressure and density respectively, and υ means kinematic viscosity.

$$\overline{u_i u_j} = \bar{u}_i \bar{u}_j + \left(\overline{u_i u_j} - \bar{u}_i \bar{u}_j\right) = \bar{u}_i \bar{u}_j - \overline{\tau_{ij}} \tag{3}$$

where $\overline{\tau_{ij}}$ means SGS Renolds stress, so equation(1) can be rewritten as

$$\frac{\partial \bar{u}_i}{\partial t} + \frac{\partial \bar{u}_i \bar{u}_j}{\partial x_j} = -\frac{1}{\rho}\frac{\partial \bar{p}}{\partial x_i} + \upsilon \frac{\partial^2 \bar{u}_i}{\partial x_j \partial x_j} + \frac{\partial \overline{\tau_{ij}}}{\partial x_j} \tag{4}$$

The subgrid scale Reynolds stress can be simulated by lots of computation patterns. Smargorinsky pattern was adopted here.

$$\overline{\tau_{ij}} = 2\upsilon_t \overline{S_{ij}} + \frac{1}{3}\delta_{ij}\overline{\tau_{kk}} \tag{5}$$

$$\upsilon_t = C_s \Delta^2 \left(2\overline{S_{ij} S_{ij}}\right)^{\frac{1}{2}} \tag{6}$$

$$\overline{S_{ij}} = \frac{1}{2}\left(\frac{\partial \bar{u}_i}{\partial x_j} + \frac{\partial \bar{u}_j}{\partial x_i}\right) \tag{7}$$

where υ_t expresses the subgrid eddy viscosity coefficient, C_s=0.18 is Smargorinsky constant and

$\overline{S_{ij}}$ is deformation rate tensor of solvable scales.

2.2 FW-H acoustic analogy

The FW-H equation is an exact rearrangement of the continuity equation and Navier-Stokes equations into the form of an inhomogeneous wave equation with two surface source terms and a volume source term. It is given as

$$\left(\frac{1}{{c_0}^2}\frac{\partial^2}{\partial t^2}-\nabla^2\right)\left({c_0}^2(\rho-\rho_0)H(f)\right)$$
$$=\frac{\partial}{\partial t}\left(\left(\rho\left(v_j-V_j\right)+\rho_0 V_j\right)\frac{\partial H}{\partial x_j}\right)-\frac{\partial}{\partial \mathrm{x}_j}\left(\left(\rho v_j\left(v_j-V_j\right)+(p-p_0)\delta_{ij}-\sigma_{ij}\right)\frac{\partial H}{\partial x_j}\right)$$
$$+\frac{\partial^2}{\partial \mathrm{x}_i\,\partial \mathrm{x}_j}\left(T_{ij}H(f)\right) \tag{8}$$

where c_0 is the sound speed, v is the flow velocity perpendicular to integer surface, V is the velocity of integer surface motion, $\sigma(f)$ is Dirac function, $H(f)$ is Heaviside function and T_{ij} is Lighthill stress tensor.

On the right side of the equation, three sound source terms represent the first monopole source term, the second dipole source term and the third quadrupoles source term, respectively. The decomposition of three sound sources terms has brought great convenience for numerical calculation since it is not necessary to consider all three source terms in acoustic problems. The monopole source and quadrupoles source are negligible and dipole the source becomes the principal sound source because of the low Mach number and the almost motionless surface.

3. COMPUTATION MODEL

3.1 Model simplification

Due to the coupling process of flow motion, heat transfer and sound generation and the complex geometry of fin-tube array, it is too difficult to establish complete model and take all factors into consideration, the computation models were simplified reasonably as follows to guarantee modeling precision and reduce computation cost.

1) The physical property of the exhaust gas can be calculated by equation of state of ideal gas according to the components of the gas. It is reasonable to take air instead of exhaust gas in the modeling process.
2) In the process of HRSG operation, it is assumed that the flow field and temperature field in HRSG are steady and the thermodynamic parameter of each heat exchanger is uniform.
3) The 3-D fin-tube array of heat exchanger in HRSG is simplified as a 2-D cylindrical tube array by follow procedure shown in Figure 2.

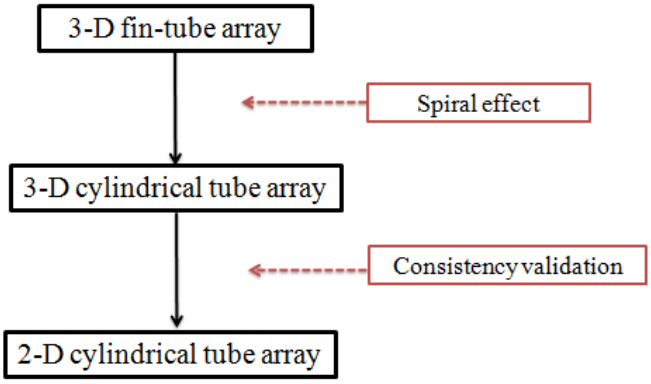

Figure 2 - Flow chart of model simplification process

3.2 Finite element models and boundary conditions

In order to investigate the mechanism of vortex noise generation, models of cylindrical tube,

fin-tube and cylindrical tube array were established respectively, as:

- Both 2-D cylindrical tube and 3-D cylindrical tube models were established to validate consistency. The computational domain extended over 15d downstream domain to make sure a steady tail flow, 5d upstream, 5d transverse and 5d height in 3-D models, where d was the diameter of the cylindrical tube. At the inlet boundary, a uniform velocity profile normal was defined and the outflow boundary condition was used at the outlet. On all solid boundaries, the no-slip conditions were imposed.
- 3-D fin-tube model was established to study the effects of the spiral fin shown in Fig. 3(a). The computational domain and the boundary conditions were the same as single cylindrical tube.
- 2-D cylindrical tube array model was established to simulate flow field and acoustic field in HRSG. It was difficult to establish a complete model of 12×64 tube array, so we took a part of the array as 12×10 with the same d as cylindrical tube. The tube array was staggeredly arranged as equilateral triangle with 2.1d between tubes. The computational domain was 25d×200d, and the same boundary conditions of inlet, outlet and tube wall were applied. For the left and right bouandary of flow domain, periodic boundary condition was defined.

The CFD mesh was built up using a non-uniform size mesh and a mesh shrunk ratio near the wall. The first layer scale near the wall was 5×10^{-3}d in order to catch the viscous stress change. The instantaneous computation time step was 0.0005s corresponds to the analysis frequency up to 1kHz.

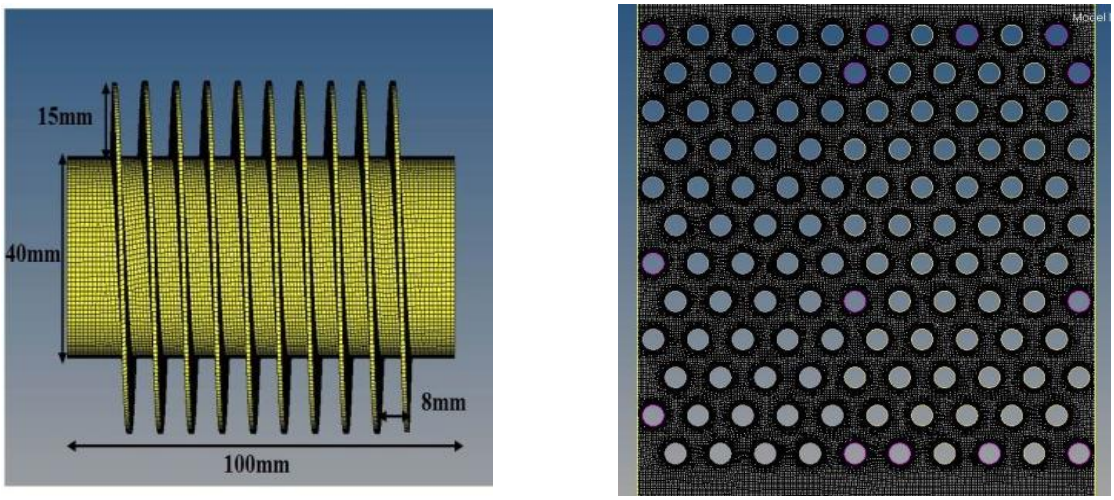

(a) Element model of fin-tube (b) Element model of tube array

Figure 3 - Computational grids of the model

3.3 Analysis conditions

There are a series of heat exchanger tube array, such as the superheater, economizer and evaporator in HRSG. The gas parameter and flow velocity of them are all different. The characteristics of aeroacoustic noise of the hot end of high pressure superheater and the cold end of deoxidizing evaporator were considered in this paper. The gas thermodynamic parameters of the concerned heat exchanger were shown in Table. 1. To study the effects of flow velocity on aeroacoustic noise, various of flow velocities(i.e. 5m/s, 10 m/s, 15 m/s, 20 m/s and 25 m/s) were applied, covering the common flow velocity range of HRSG operation.

Table 1 -Thermodynamic parameters of gas

	Temperature	Density	Viscosity	Sound Speed
High Pressure Superheater(HPS)	517℃	0.457kg m-3	3.72E-05 Pa s	554.6m s-1
Deoxidizing Evaporator(DE)	128℃	0.894kg m-3	2.32E-05 Pa s	401.1m s-1

4. RESULTS AND DISCUSSION

The vorticity distribution in the middle section of different models in high pressure superheater

condition at flow velocity of 10m s-1 was shown in Figure 4. From Figure 4 the vortex shedding phenomenon is obvious. The sound pressure levels of different models in high pressure superheater condition at different flow velocities shown in Figure5 suggest that the aeroacoustic noise deriving from vortex shedding has significant low frequency peak, which is the characteristic frequency we concerned.

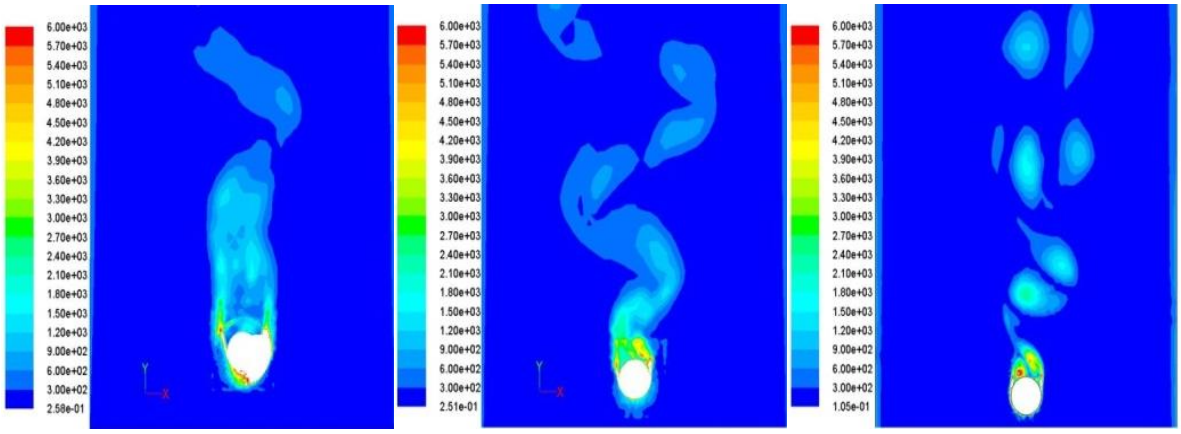

(a)fin-tube (b)3-D cylindrical tube (c) 2-D cylindrical tube

Figure 4 - Vorticity distribution in middle section of different models in HPS

The aeroacoustic noise characteristic frequencies and magnitudes with different gas parameters at different flow velocities were compared. The trends of the characteristic frequencies of cylindrical tube and fin-tube with different gas parameters changing with flow velocity were shown in Figure 6 From Figure 6, there is a good linear relationship between the characteristic frequency and flow velocity. The difference of gas parameters has no effect on the characteristic frequency. The results of single cylindrical tube in 2-D and 3-D models show good consistency, so the 3-D tube array might be simplified as the 2-D array considering characteristic frequency. The fin-tube has lower characteristic frequency than the cylindrical tube, which needs more attention.

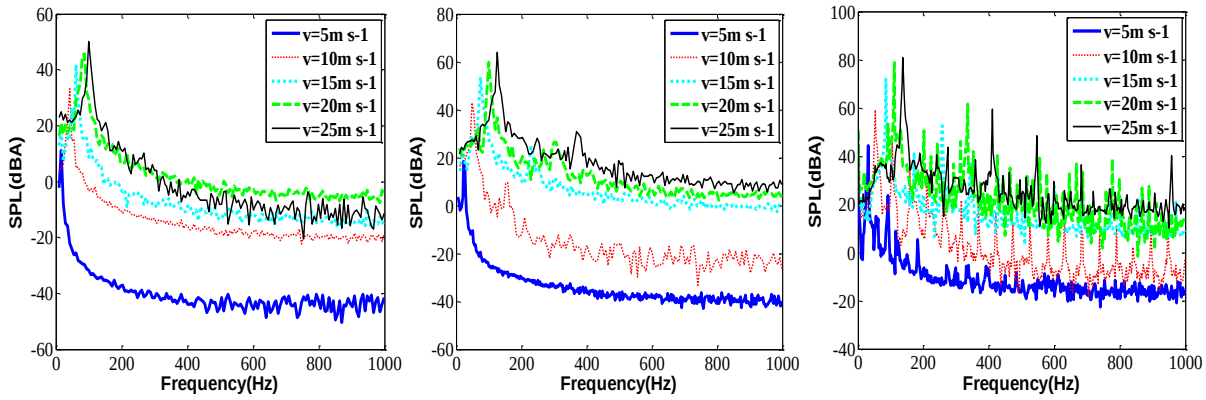

(a)fin-tube (b)3-D cylindrical tube (c) 2-D cylindrical tube

Figure 5 - Sound pressure level of different models in HPS at different flow velocity

The characteristic frequency is defined as

$$f = St\frac{v}{d} \tag{9}$$

where St is Strouhal number, v is flow velocity and d is the effective diameter. St can be regarded as constant with Re ranging from $1 \times 10^3 \sim 1 \times 10^5$, so the characteristic frequency would be linear to the flow velocity in theory when d is defined in the rang(6,7). In this simulation, Re of the gas ranges from $2.5 \times 10^3 \sim 1.25 \times 10^4$ and the results have a good agreement with the theoretical ones, which the characteristic frequency of both cylindrical tube and fin-tube is linear to the flow velocity. Therefore the frequency shifting-down phenomenon can be explained by the effective diameter of the tube, accounting for the presence of fins on the tubes. The effective diameters of fin-tube at different flow velocities are shown in Figure 7. From Figure 7, the effective diameter could be supposed to have nothing to do with flow velocity within a certain range or the gas parameter. It is

only determined by geometry, which provides the basis for fin-tube array simplified to cylindrical tube array only considering characteristic frequency. It can be an appropriate engineering approximation to use the concept of effective diameter.

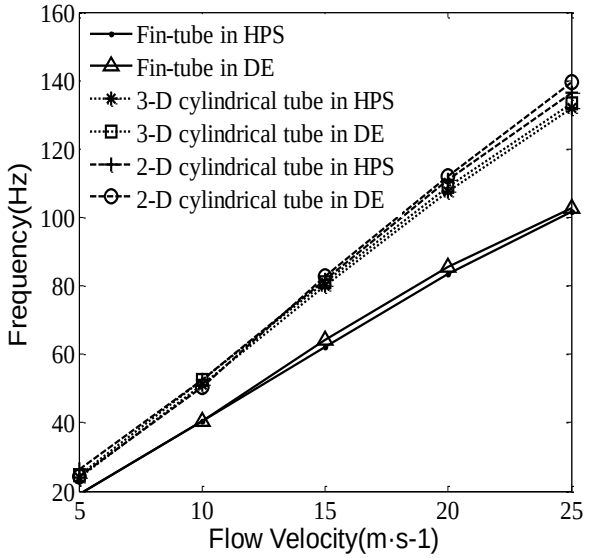

Figure 6 - The characteristic frequency of different models with different gas parameters changing with flow velocity

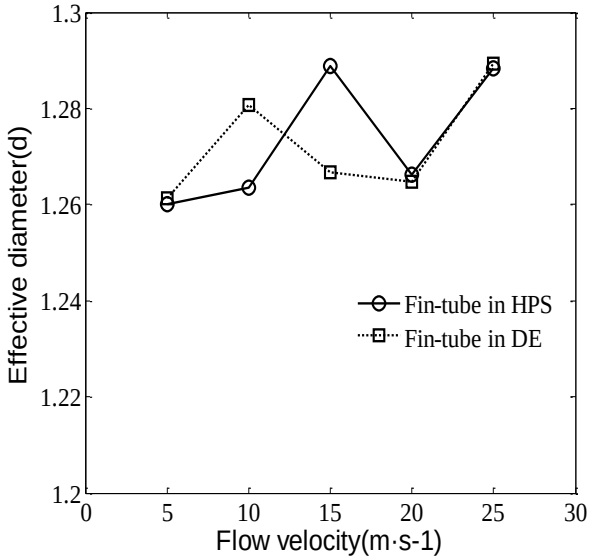

Figure 7.-. The effective diameter of fin-tube with different gas parameters changing with flow velocity

The trend of the overall sound pressure level of cylindrical tube and fin-tube with different gas parameters changing with flow velocities are shown in Figure8. It indicates that the magnitude of aeroacoustic noise is positively correlation with flow velocity and affected by gas parameter. The overall sound pressure level of the lower temperature gas is 3~7dB higher than the higher temperature gas. There is a big difference between the magnitude of 2-D cylindrical tube model and that of 3-D cylindrical tube model, the possible reason might be that the sound correlation length has to be chosen properly in 2-D computation model to simulate sound source accurately, but it is difficult to be predicted in practice. It means that the magnitude of noise of 2-D models is only the relative reference value. The spiral fin reduces the total sound pressure level of aeroacoustic noise by 10~12dB comparing with single cylindrical tube.

Vorticity distribution in middle section of tube array in high pressure superheater condition is shown in Figure 9. Vortex shedding can be observed regularly at the tube near the inlet. Differing from single cylindrical tube , the flow field becomes complicated along the flow direction because of the vortex shedding and attachment between tubes.

Figure 10 shows that the vortex noise in different rows of the tube array has obvious low-frequency characteristics, and the characteristic frequency increases from 94.9Hz to 97.9Hz along the flow direction. The frequency shifting-up phenomenon arises from the enhanced interaction of the flow field between tubes. It indicates that the vortex noise of tube array is narrowband noise with bandwidth ranging from 94.9Hz to 97.9Hz instead of the single tone frequency. The noise of tube array in deoxidizing evaporator condition has the same trend as that in high pressure superheater. However, it is negligible because the low flow velocity reduce the SPL of noise by more than 15 dB.

Considering the effects of spiral fin , the characteristic frequency band of vortex noise of tube array in high pressure superheater condition can be modified as 73.6Hz~76.1Hz by the effective diameter method. It has a good agreement with the measured results, which has a frequency band of 74Hz~78Hz.

Comparison between the numerical simulation results of vortex noise and the measurement of regeneration noise is shown in Figure 11. They have a highly consistent trend and the same octave characteristic frequency band centred at 63Hz. Despite the absolute values of SPL are incomparable due to 2-D simulation method, it is convincing proof that vortex noise is the main sound source of low frequency noise of HRSG.

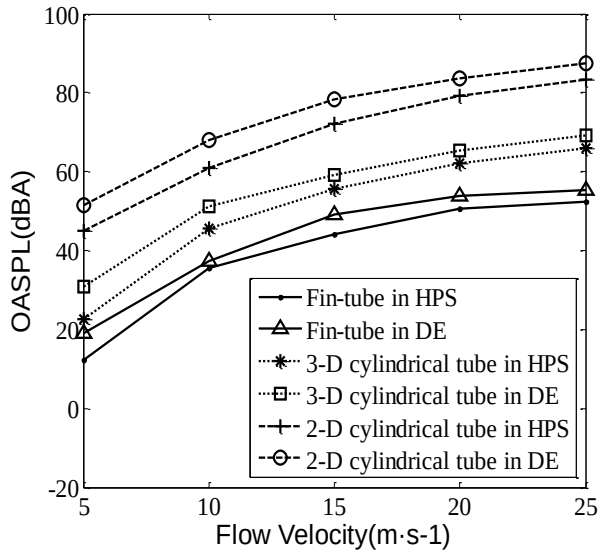

Figure 8 - The overall sound pressure level of different models with different gas parameter changing with flow velocity

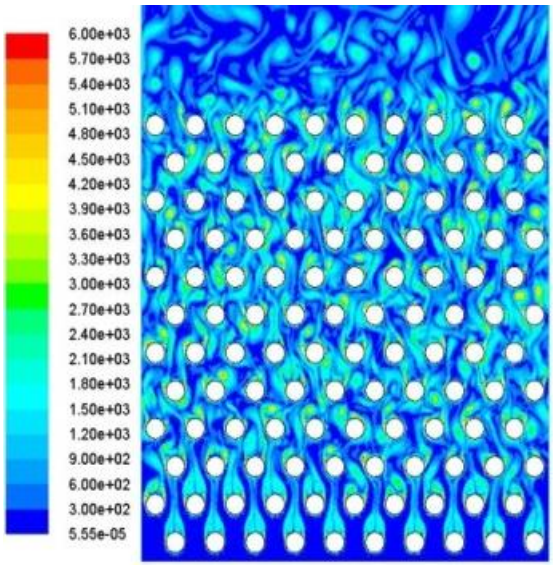

Figure 9 - Vorticity distribution in middle section of tube array in HPS

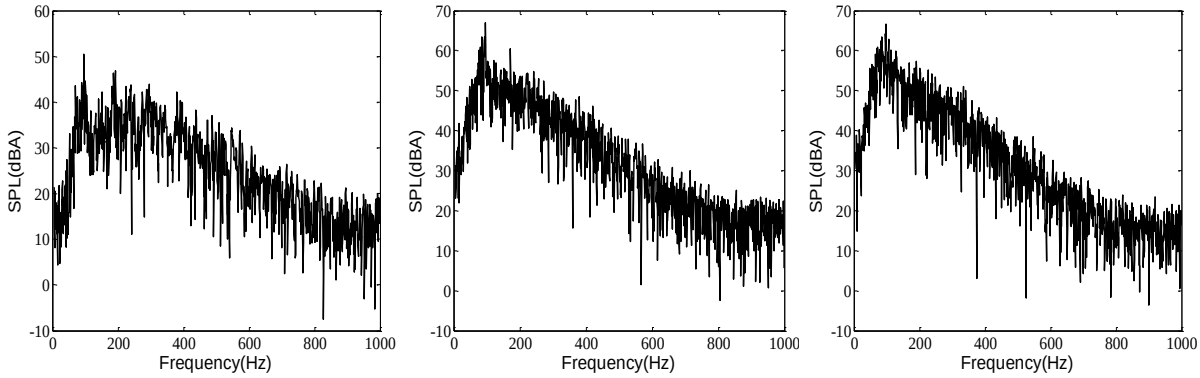

(a)1st row (b)7th row (c)12th row

Figure 10 – SPL spectrum of vortex noise in different rows of the tube array

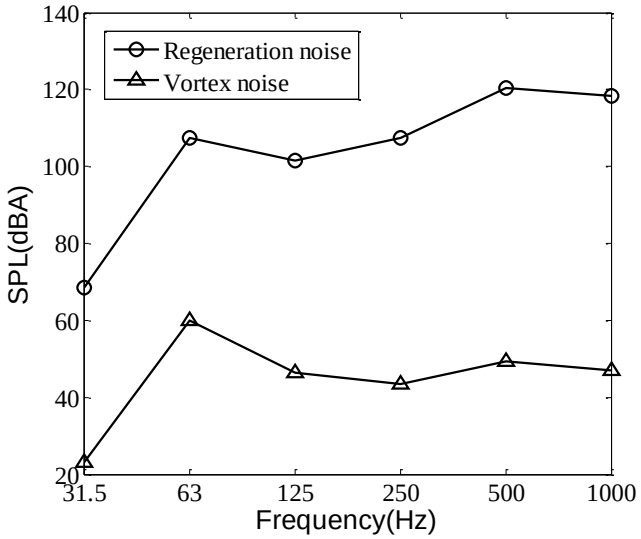

Figure 11 – Comparison between simulation results and measured results

5. CONCLUSIONS

Based on Large Eddy Simulation and Ffowcs Williams-Hawkings equation, the low frequency noise of HRSG was investigated. In order to understand the mechanism and characteristics of the noise, a series of computation models were established. Several important conclusions were drawn from the analysis:

It was understood based on experimental analysis that the low frequency noise of HRSG is mainly derived from vortex noise of heat exchanger tube array .The flow past the heat exchanger tube array will induce vortex shedding which results in the low frequency noise in dipole source terms.

The vortex noise of a cylindrical tube has the obvious characteristic tone frequency same as the vortex shedding frequency, and the spiral fin reduces the characteristic frequency and sound level. For the tube array, due to the enhanced interaction of the flow field between tubes, the vortex noise is narrowband noise with some bandwidth.

According to the research results, more targeted methods, such as optimizing the arrangement of tube array and parameters of fin-tube, or installing muffler at the exhaust end, can be used for noise reduction of HRSG.

REFERENCE

1. R. Hetzel, A Case Study of the Attenuation of Waste Heat Boiler Low Frequency Resonance. In Proceedings of Inter-Noise 2000, I-INCE and SFA InterNoise 2000, Nice, France, 2000.
2. Robert A. Putnam. Low frequency noise from heat recovery steam generators. Inter-noise 2006, HONOLULU, HAWAII, USA, Dec3-6, 2006.
3. Kenneth S. Brentner , Christopher L. Rumsey. Computation of Vortex Shedding and Radiated Sound for a Circular Cylinder Subcritical to Transcritical Reynolds Numbers. Theoretical and Computational Fluid Dynamics, 1998, 12: 233-253.
4. TANG Ke-fan, Franke J. Numerical simulation of noise induced by flow around cylinder using the hybrid method with the solutions of NS equation and FW-H integration.Chinese Journal of hydrodynamics, 2009, 02: 190-199.
5. YU Lei, SONG Wen-ping, HAN Zhong-hua, etc. Aeroacoustic noise prediction using hybrid RANS/LES method and FW-H Equation. Acta Aeronautica et Astronautica Sinica, 2013, 08: 1795-1805.
6. Blevins, R. D., "Flow-Induced Vibration" 2nd. Ed. 1990, Van Nostrand Reinhold, New York, NY.
7. Fitzhugh, J. S. (1973) "Flow Induced Vibration in Heat Exchangers", Oxford University Report RS57 (AERE P7238).